J. Fluid Mech. (1981), *vol.* 105, *pp.* 347–368
Printed in Great Britain

Mixed convection in a two-dimensional buoyant plume

By NOOR AFZAL
Department of Mechanical Engineering, Aligarh Muslim University, Aligarh, India

(Received 24 September 1979 and in revised form 14 May 1980)

The mixed convection in a two-dimensional line heat source is studied for the situations where buoyancy effects are favourable or adverse with respect to the oncoming vertical stream. The problem is analysed in terms of two co-ordinate expansions, direct and inverse, valid for small and large values of streamwise distance from the heat source. The solution for the first eleven and seven terms in direct and inverse co-ordinate expansions, respectively, are obtained. The direct expansion, when suitably transformed by Euler transformation and other techniques, predicts the velocity and temperature to two-digit accuracy for all values of streamwise co-ordinates, with a maximum error of 0·1 % for velocity, 0·8 % for temperature and 2·2 % for displacement thickness far downstream from the source.

1. Introduction

The mixed convection in a buoyant plume due to a two-dimensional heat source is of interest in several engineering applications, e.g. hot-wire anemometry, dispersion of pollutants. The problem for a weakly buoyant plume has been studied by Wood (1972) and Wesseling (1975). This paper presents a complete solution describing the entire flow regime ranging from weakly to strongly buoyant plumes.

In the study of Wood (1972), for mixed convection in a weakly buoyant plume where the free stream is directed vertically upwards, the Oseen linearization of boundary-layer equations has been employed. The explicit closed-form solution has been obtained for the first-order terms in the expansion valid near the source.

Wesseling (1975) for weakly buoyant plumes has considered the leading term in the Oseen linearization of Navier–Stokes equations in the neighbourhood of a horizontal line source of heat and the free stream is directed at an arbitrary angle with respect to the buoyancy force vector. He has shown that the Oseen-approximation does not admit solutions with a uniform pressure at infinity, except for a vertically upward stream. Wesseling noted that the situation is analogous to the Stokes paradox. The paradox raised by Wesseling has already been resolved in Wood's earlier paper who has shown that this singularity in the pressure, and the associated singularities in the velocity, fit naturally into a wider picture of the flow which includes the nonlinear development of the buoyant plume at distances from the heat source larger than that at which the Oseen-linearized equations hold. Away from the heat source there is a region where buoyancy and forced convection effects are of comparable magnitude, the Oseen linearization fails and one has to consider the full nonlinear equations. At sufficiently large distances from the heat source the problem is governed mainly by buoyancy and the asymptotic solution corresponds to that given by Fuji (1963).

The aim of the present work is to study the nonlinear mixed convection in the buoyant plume due to a horizontal line source of heat in a vertical stream for the two situations when buoyancy effects with respect to the vertical stream are positive and negative, i.e. upward and downward flows. The plume is taken as thin so that the boundary-layer equations can describe the flow to a good approximation. The two physically extreme situations of purely forced and free convections yield two different similarity variables. For the present problem the solutions have been developed in terms of two co-ordinate expansions: a direct co-ordinate expansion for a weakly buoyant plume valid for small streamwise distance from the source and an inverse co-ordinate expansion for strongly buoyant plume valid for very large distance from the source. The solutions to the first eleven terms in direct co-ordinate expansion and a first seven terms in inverse co-ordinate expansion have been obtained. It is shown that if the series for a weakly buoyant plume is suitably transformed it can describe very accurately the entire domain of the flow.

2. Governing equations

We consider the flow past a two-dimensional horizontal line source of heat in a vertical uniform stream of the fluid at upstream infinity with velocity U_∞ and temperature T_∞. The boundary-layer equations for the flow, under Boussinesq approximation, are

$$\frac{\partial u}{\partial x}+\frac{\partial v}{\partial y}=0, \tag{1}$$

$$u\frac{\partial u}{\partial x}+v\frac{\partial u}{\partial y}=\nu\frac{\partial^2 u}{\partial y^2}\pm g\beta(T-T_\infty), \tag{2}$$

$$u\frac{\partial T}{\partial x}+v\frac{\partial T}{\partial y}=\frac{\nu}{\sigma}\frac{\partial^2 T}{\partial y^2}. \tag{3}$$

The positive sign with the buoyancy term corresponds to the favourable case where buoyancy accelerates the flow in the plume and the negative sign to the adverse case where buoyancy retards the flow in the plume. Here x is the vertical co-ordinate measured from the heat source and y is normal to it. u and v are the velocity components in the x and y directions respectively and T is the temperature. The ν is the kinematic viscosity of the fluid, g the gravitational acceleration, β the volumetric thermal expansion coefficient and σ the Prandtl number of the fluid. The velocity and temperature distributions must be symmetrical with respect to the vertical x axis,

$$v=\frac{\partial u}{\partial y}=\frac{\partial T}{\partial y}=0, \quad y=0. \tag{4}$$

Sufficiently far away from the heat source the velocity and temperature of the fluid are not affected:

$$u\to U_\infty, \quad T\to T_\infty, \quad y\to\infty. \tag{5}$$

An integration of energy equation within the mixed convection region yields

$$C_p\int_{-\infty}^{\infty}u(T-T_\infty)\,dy=Q, \tag{6}$$

where Q is the heat released from the thermal source. The displacement thickness δ^* of the buoyant plume is given by

$$\delta^* = \frac{g\beta Q}{\rho C_p \nu U_\infty^2} \int_0^\infty 1 - \frac{u}{U_\infty} dy. \tag{7}$$

3. Weakly buoyant plume

Near the heat source the boundary layer is formed mainly by forced convection flow affected by buoyancy. The effects of buoyancy force increase as the boundary layer develops from the heat source. Thus in the region near the source the forced convection is dominant and the flow will behave like a two-dimensional wake. We consider the following variables

$$\psi = (\nu U_\infty x)^{\frac{1}{2}} F(\xi, \zeta), \quad T - T_\infty = \theta_T (U_\infty x/\nu)^{-\frac{1}{2}} H(\xi, \zeta). \tag{8}$$

The variables ξ and η are defined by

$$\xi = Gr_x / R_x^{\frac{5}{2}} = g\beta\theta_T \left(\frac{\nu x}{U_\infty^5}\right)^{\frac{1}{2}}, \quad \zeta = y \left(\frac{U_\infty}{\nu x}\right)^{\frac{1}{2}}, \tag{9}$$

where Gr_x is the local Grashof number, R_x the local Reynolds number and θ_T are defined by

$$Gr_x = \frac{g\beta\theta_T x^3}{\nu^2}, \quad R_x = \frac{U_\infty x}{\nu}, \quad \theta_T = \frac{Q}{\rho C_p \nu}. \tag{10}$$

Now the equations (1) to (3) reduce to

$$F_{\zeta\zeta\zeta} + \tfrac{1}{2} F F_{\zeta\zeta} \pm \xi H = \tfrac{1}{2}\xi (F_\zeta F_{\xi\zeta} - F_{\zeta\zeta} F_\xi), \tag{11}$$

$$\sigma^{-1} H_{\zeta\zeta} + \tfrac{1}{2}(FH)_\zeta = \tfrac{1}{2}\xi (F_\zeta H_\xi - H_\zeta F_\xi). \tag{12}$$

The corresponding boundary and integral heat flux conditions are

$$F = 0, \quad F_{\zeta\zeta} = H_\zeta = 0, \quad \zeta = 0, \tag{13a}$$

$$F_\zeta \to 1, \quad H \to 0, \quad \zeta \to \infty, \tag{13b}$$

$$\int_{-\infty}^{\infty} F_\zeta H \, d\zeta = 1. \tag{14}$$

The method of solution is to expand the variables in powers of ξ:

$$F(\xi, \zeta) = \sum_{n=0}^{\infty} (\pm\xi)^n F_n(\zeta), \quad H(\xi, \zeta) = \sum_{n=0}^{\infty} (\pm\xi)^n H_n(\zeta). \tag{15}$$

The solution governing the equations for leading approximation ($n = 0$) subject to the boundary conditions and that of heat flux is

$$F_0 = \zeta, \quad H_0 = \left(\frac{\sigma}{4\pi}\right)^{\frac{1}{2}} \exp\left(-\frac{\sigma}{4}\zeta^2\right). \tag{16}$$

The equations governing the higher-order terms $n \geqslant 1$ in the series (15) can be written in terms of recurrence relations

$$F_n''' + \tfrac{1}{2}\zeta F_n'' - \frac{n}{2} F_n' = -H_{n-1} + \frac{1}{2}\sum_{r=1}^{n-1} [r F_r' F_{n-r}' - (r+1) F_r F_{n-r}''], \tag{17}$$

$$\sigma^{-1} H_n'' + \tfrac{1}{2}\zeta H_n' + \frac{1-n}{2} H_n + \frac{1+n}{2} F_n H_0' + \tfrac{1}{2} F_n' H_0 = \frac{1}{2}\sum_{f=1}^{n-1} [(r-1) H_r F_{n-r}' - (r+1) F_r H_{n-r}'], \tag{18}$$

together with the boundary and integral conditions

$$F_n(0) = F_n''(0) = H_n'(0) = F_n'(\infty) = H_n(\infty) = 0, \tag{19}$$

$$\int_{-\infty}^{\infty} F_n' H_0 + F_0' H_n + \sum_{r=1}^{n-1} F_r' H_{n-r}\, d\zeta = 0. \tag{20}$$

The expression (7) for displacement thickness δ^* becomes

$$\delta^* = \int_0^{\infty} 1 - F_\zeta d\zeta = -\sum_{n=1}^{\infty} F_n(\infty)(\pm\xi)^n. \tag{21}$$

The solution to the equation for F_1 when $\sigma = 1$ is

$$F_1 = \tfrac{1}{2}\operatorname{erf}(\tfrac{1}{2}\zeta) \tag{22a}$$

and when $\sigma \neq 1$ is

$$F_1 = \frac{\sigma}{4(\sigma-1)}\left[(\zeta^2+2)\operatorname{erf}(\tfrac{1}{2}\zeta) - (\zeta^2 + 2/\sigma)\operatorname{erf}(\tfrac{1}{2}\sigma^{\frac{1}{2}}\zeta) + \frac{2\zeta}{\sqrt{\pi}}\left\{\exp(-\tfrac{1}{4}\zeta^2) - \frac{1}{\sigma^{\frac{1}{2}}}\exp(-\tfrac{1}{4}\sigma\zeta^2)\right\}\right]. \tag{22b}$$

The perturbation velocity at the axis is given by

$$F_1'(0) = \frac{(\sigma/\pi)^{\frac{1}{2}}}{1+\sigma^{\frac{1}{2}}}. \tag{23}$$

The solution of Wood (1972) for F_1 is

$$F_1' = \frac{2\pi^{\frac{1}{2}}|\zeta|}{\sigma-1}\int_{|\zeta|}^{\infty}\left\{\exp(-\tfrac{1}{4}\zeta^2) - \frac{1}{\sigma^{\frac{1}{2}}}\exp(-\tfrac{1}{4}\sigma\zeta^2)\right\}\zeta^{-2}\, d\zeta, \tag{24}$$

and corresponds to a normalizing condition different from (14).

The equation to the next-order energy equation can also be solved in the form to yield for $\sigma = 1$

$$H_1 = \frac{1}{16\pi}[\pi - 4\exp(-\tfrac{1}{2}\zeta^2) - \pi\operatorname{erf}^2(\tfrac{1}{2}\zeta) - 2\zeta\pi^{\frac{1}{2}}\exp(-\tfrac{1}{4}\zeta^2)\operatorname{erf}(\tfrac{1}{2}\zeta)], \tag{25}$$

and when $\sigma \neq 1$

$$H_1 = \frac{\sigma^{\frac{3}{2}}\exp(-\frac{1}{4}\sigma\zeta^2)}{32\pi(\sigma-1)}\left[\pi^{\frac{1}{2}}(\sigma\zeta^3+6\zeta)\operatorname{erf}(\tfrac{1}{2}\sigma^{\frac{1}{2}}\zeta) - \pi^{\frac{1}{2}}\{\sigma\zeta^3 + (4\sigma+2)\zeta\}\operatorname{erf}(\tfrac{1}{2}\zeta) - 2(2\sigma+2+\zeta^2)\exp(-\tfrac{1}{4}\zeta^2) + \frac{2}{\sigma^{\frac{1}{2}}}(4+\sigma\zeta^2)\exp(-\tfrac{1}{4}\sigma\zeta^2)\right] + \frac{\sigma^{\frac{3}{2}}}{8\pi^{\frac{1}{2}}}(\sigma+1)J(\sigma, \tfrac{1}{2}\zeta). \tag{25}$$

The function $J(\sigma, x)$ is an integral defined by

$$J(\sigma, x) = \int_x^\infty \exp(-\sigma\zeta^2)\,\mathrm{erf}(\zeta)\,d\zeta. \tag{26}$$

Using the following results from Erdélyi (1953)

$$\int_0^\infty e^{-st}t^{\beta-1}\gamma(\alpha, t)\,dt = \frac{\Gamma(\alpha+\beta)}{\alpha(1+s)^{\alpha+\beta}}\{{}_2F_1(1, \alpha+\beta, \alpha+1, 1/[1+s])\}, \tag{27a}$$

$${}_2F_1(1, 1, \tfrac{3}{2}, \sin^2\alpha) = \frac{\alpha}{\sin\alpha\cos\alpha}, \tag{27b}$$

where ${}_2F_1$ is the hypergeometric function and $\gamma(\alpha, t)$ the incomplete gamma function; the value of the integral at $\zeta = 0$ can be estimated as

$$J(\sigma, 0) = \frac{1}{(\pi\sigma)^{\frac{1}{2}}}\tan^{-1}\left(\frac{1}{\sigma^{\frac{1}{2}}}\right).$$

The perturbation temperature at the axis is given by

$$H_1(\sigma) = \frac{\sigma(\sigma+1)}{8\pi}\left[\tan^{-1}\left(\frac{1}{\sigma^{\frac{1}{2}}}\right) - \frac{\sigma+\sigma^{\frac{1}{2}}+2}{(1+\sigma)(1+\sigma^{\frac{1}{2}})}\right]. \tag{28}$$

The analytical solution of further higher-order equations in the set of equations (17)–(20) is very laborious. Therefore, the solutions to the first eleven terms in the series for velocity and temperature have been obtained numerically for $\sigma = 0{\cdot}72$ and results are presented in § 5.

4. Strongly buoyant plume

Away from the heat source the buoyancy force affects the flow in an appreciable manner. Asymptotically far away from the source where the boundary layer is mainly governed by buoyancy, the flow in the favourable case approaches a limit corresponding to the purely free convection buoyant plume. For this case we consider the following variables

$$\eta = Gr_x^{\frac{1}{5}}\,y/x, \quad \epsilon = \xi^{-\frac{2}{5}},$$
$$\psi = Gr_x^{\frac{1}{5}}f(\epsilon, \eta), \quad t = \theta_T Gr_x^{-\frac{1}{5}}h(\epsilon, \eta). \tag{29}$$

These variables (29) are connected to earlier variables (8) and (9) by the relations

$$\eta = \zeta/\epsilon^{\frac{1}{5}}, \quad f = \epsilon^{\frac{1}{5}}F, \quad h = H/\epsilon^{\frac{1}{5}}. \tag{30a, b, c}$$

Introducing the variables (29) in the governing equations, we get

$$f_{\eta\eta\eta} + \tfrac{3}{5}ff_{\eta\eta} - \tfrac{1}{5}f_\eta^2 + h = \tfrac{1}{5}\epsilon(f_\eta f_{\eta\epsilon} - f_\epsilon f_{\eta\eta}), \tag{31}$$

$$\sigma^{-1}h_{\eta\eta} + \tfrac{3}{5}(fh)_\eta = \tfrac{1}{5}\epsilon(f_\eta h_\epsilon - f_\epsilon h_\eta). \tag{32}$$

The boundary conditions are

$$\eta = 0, \quad f = f_{\eta\eta} = h_\eta = 0, \tag{33}$$

$$\eta \to \infty, \quad f_\eta \to \epsilon, \quad h \to 0, \tag{34}$$

subject to heat flux condition

$$\int_{-\infty}^{\infty} f_\eta h \, d\eta = 1. \tag{35}$$

The expression (7) for δ^* becomes

$$\delta^* = \xi^{\frac{8}{5}} \int_0^{\infty} \epsilon - f_\eta \, d\eta. \tag{36}$$

When ϵ is small the boundary condition (34a) suggests that the solution can be written in terms of power series in ϵ. It may, however, be noted that such an expansion in ϵ would essentially be an inverse co-ordinate expansion as $\epsilon \propto x^{-\frac{1}{5}}$. It is well known that the inverse co-ordinate expansions suffer from the indeterminacy (Van Dyke 1964) which gives rise to the eigensolutions. This indeterminacy physically represents the uncertainty about the detail of the flow near the heat source and arises from the fact that the initial conditions are not imposed on the similarity solutions. It can be easily shown that the present problem has an infinite set of discrete eigenfunctions given by

$$\psi^{(m)} = C_m \epsilon^{-3-m} \tilde{f}_m(\eta), \tag{37a}$$

$$h^{(m)} = C_m \epsilon^{3-m} \tilde{h}_m(\eta), \tag{37b}$$

where the C_m's are unspecified eigenconstants which in some way are associated with the upstream conditions.

In an asymptotic expansion for small values of ϵ the first eigenvalue ($m = 5$) occurs at a stage for which a particular integral, in the sixth-order term, is required and the condition of exponential decay cannot be fulfilled unless the additional term, consisting of complementary function multiplied by $\ln \epsilon$, is added to the asymptotic expansions. The numerical factor in this term is to be determined by the condition that the particular integral be exponentially small when η is large. Thus we consider the following expansions

$$f(\epsilon, \eta) = \sum_{m=0}^{4} \epsilon^m f_m(\eta) + \epsilon^5 \ln \epsilon \, \tilde{f}_5(\eta) + \epsilon^5 f_5(\eta) + o(\epsilon^5), \tag{38}$$

$$h(\epsilon, \eta) = \sum_{m=0}^{4} \epsilon^m h_m(\eta) + \epsilon^5 \ln \epsilon \, \tilde{h}_5(\eta) + \epsilon^5 h_5(\eta) + o(\epsilon^5). \tag{39}$$

The leading term of the expansions is governed by the equations

$$f_0''' + \tfrac{3}{5} f_0 f_0'' - \tfrac{1}{5} f_0'^2 + h_0 = 0, \quad \sigma^{-1} h_0'' + \tfrac{3}{5} (f_0 h_0)' = 0,$$

$$f_0(0) = f_0''(0) = h_0'(0) = f_0'(\infty) = h_0(\infty) = 0, \quad \int_{-\infty}^{\infty} f_0' h_0 \, d\eta = 1 \tag{40}$$

of a two-dimensional buoyant plume (Fuji 1963).

The next set of equations may be written in terms of two operators defined by

$$L(f_m, h_m) = f_m''' + \tfrac{3}{5} f_0 f_m'' + \frac{m-2}{5} f_0' f_m' + \frac{3-m}{5} f_0'' f_m + h_m, \tag{41}$$

$$\mathscr{L}(f_m, h_m) = \sigma^{-1} h_m'' + \tfrac{3}{5} f_0 h_m' + \frac{3+m}{5} f_0' h_m + \frac{3-m}{5} f_m h_0' + \tfrac{3}{5} f_m' h_0. \tag{42}$$

The equations for the next four orders in ϵ ($m = 1, 2, 3, 4$) are

$$L(f_m, h_m) = R_m, \quad \mathscr{L}(f_m, h_m) = \mathscr{R}_m, \tag{43), (44}$$

$$5R_m = -\sum_{r=1}^{m-1} [(3-r) f_r f''_{m-r} + (r-1) f'_r f'_{m-r}], \tag{45}$$

$$5\mathscr{R}_m = \sum_{r=1}^{m-1} [(3+r) h_r f'_{m-r} + (3-r) f'_r h'_{m-r}], \tag{46}$$

$$f_m(0) = f''_m(0) = h'_m(0) = h_m(\infty) = 0, \quad f'_m(\infty) = \delta_{2m}, \tag{47}$$

$$\int_{-\infty}^{\infty} \sum_{r=0}^{m} f'_r h_{m-r}\, d\eta = 0, \tag{48}$$

where δ_{2m} is the well-known Kronecker delta. The solution to the equation for $\tilde{f}_5$ and $\tilde{h}_5$ is

$$\tilde{f}_5 = c_1(\tfrac{3}{2} f_0 - \eta f'_0), \quad \tilde{h}_5 = -c_1(\tfrac{3}{2} h_0 + \eta h'_0), \tag{49a, b}$$

where c_1 is an unspecified constant. The equations for terms of order ϵ^5 are

$$L(f_5, h_5) = R_5 + \tfrac{1}{5}(-\tilde{f}_5 f''_0 + f'_0 \tilde{f}'_5) = R_5 + \frac{c_1}{10}(3 f_0 f''_0 - f'^2_0), \tag{50}$$

$$\mathscr{L}(f_5, h_5) = \mathscr{R}_5 + \tfrac{1}{5}(-\tilde{f}_5 h'_0 + f'_0 \tilde{h}_5) = \mathscr{R}_5 + \frac{c_1}{10}(3 f'_0 h_0 - 3 f_0 h'_0), \tag{51}$$

$$f_5(0) = f''_5(0) = h'_5(0) = f'_5(\infty) = h_5(\infty) = 0, \tag{52}$$

$$\int_{-\infty}^{\infty} \sum_{r=0}^{5} f'_r h_{5-r} + f'_0 \tilde{h}_5 + \tilde{f}'_5 h_0\, d\eta = 0. \tag{53}$$

The solution to the seven terms is obtained numerically as a two-point boundary-value problem for $\sigma = 0{\cdot}72$. The seventh-order equations (50)–(53) involve a constant c_1 and a method for its determination, given in the appendix, yields $c_1 = 1{\cdot}0728$.

5. Results and discussion

The problem of mixed convection above a two-dimensional line source of heat, in general, does not admit self-similarity, except in two asymptotically different situations of pure forced and pure free convections. For these two situations a direct co-ordinate expansion valid for weakly buoyant plumes and an inverse co-ordinate expansion for strongly buoyant plumes are developed. The ordinary differential equations are integrated numerically by the Runge–Kutta–Gill method on IBM 1130 computer. For automatic calculations of higher-order approximations the recursive relations (17)–(20) for successive equations in low ξ perturbation series is programmed mainly as nested 'do' loops. The solutions to the first eleven terms in the direct co-ordinate expansion and the first seven terms in the inverse co-ordinate expansion are obtained for air ($\sigma = 0{\cdot}72$).

We first present our results for strongly buoyant flows analysed in § 4. The numerical

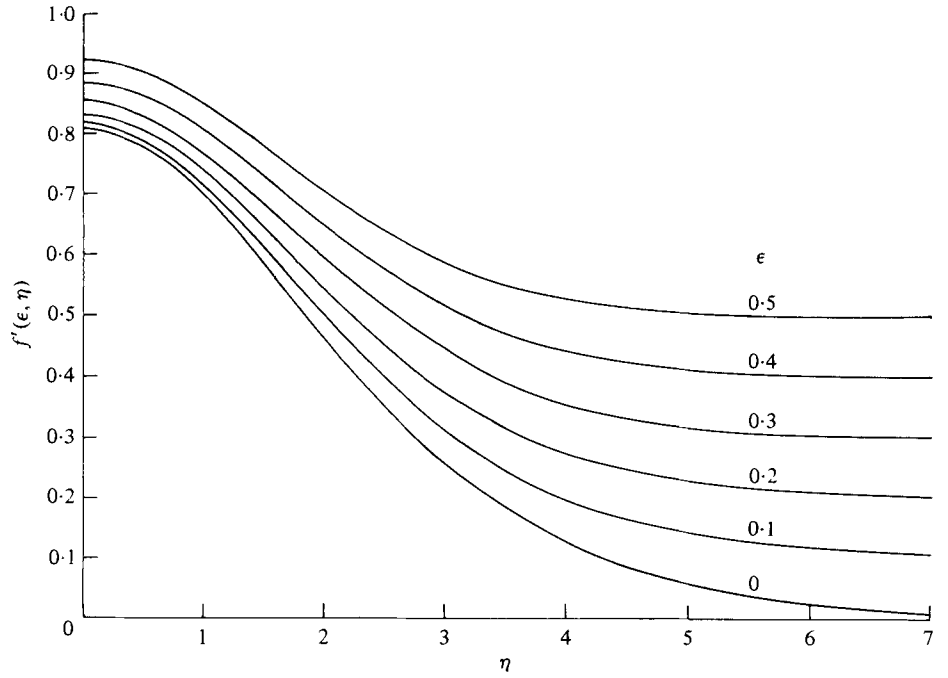

FIGURE 1. Favourable case: the velocity profiles from the first five terms of series (38) for a strongly buoyant plume.

results for the first seven terms for velocity, temperature in the plane of symmetry and displacement thickness for strongly buoyant plume are given below,

$$f'(\epsilon, 0) = 0{\cdot}8096 + 0{\cdot}0631\epsilon + 0{\cdot}2235\epsilon^2 + 0{\cdot}1834\epsilon^3 + 0{\cdot}03886\epsilon^4 - 0{\cdot}4077\epsilon^5 \ln\epsilon + (-1{\cdot}0338 + 0{\cdot}8096\lambda)\epsilon^5 + o(\epsilon^5), \tag{54a}$$

$$h(\epsilon, 0) = 0{\cdot}3773 - 0{\cdot}1893\epsilon - 0{\cdot}008598\epsilon^2 + 0{\cdot}1132\epsilon^3 - 0{\cdot}06389\epsilon^4 + 0{\cdot}6071\epsilon^5 \ln\epsilon - 0{\cdot}3773\lambda\epsilon^5 + o(\epsilon^5), \tag{54b}$$

$$\delta^* = \xi^{\frac{6}{5}}[-2{\cdot}0441 + 3{\cdot}1440\epsilon - 2{\cdot}1141\epsilon^2 + 1{\cdot}8914\epsilon^3 - 3{\cdot}5380\epsilon^4 + 3{\cdot}2894\epsilon^5 \ln\epsilon + (11{\cdot}8579 - 6{\cdot}1322\lambda)\epsilon^5 + o(\epsilon^5)]. \tag{54c}$$

The methods of determining the coefficient of the logarithmic term in the above expansions is described in the appendix. These results suffer from indeterminacy, as it involves an unspecified constant λ in the seventh term. For computational purposes, however, the sixth and seventh terms are to be treated together (Van Dyke 1964). The first five terms of the series (54) show that their convergences are good only for $\epsilon \lesssim 0{\cdot}4$ or $\xi \gtrsim 10$. The velocity and temperature profiles for a strongly buoyant plume obtained from the first five terms of the series (38) and (39) for various values of ϵ are displayed in figures 1 and 2. The characteristic values (54) are displayed in figure 5 and the discussion of the results is presented later.

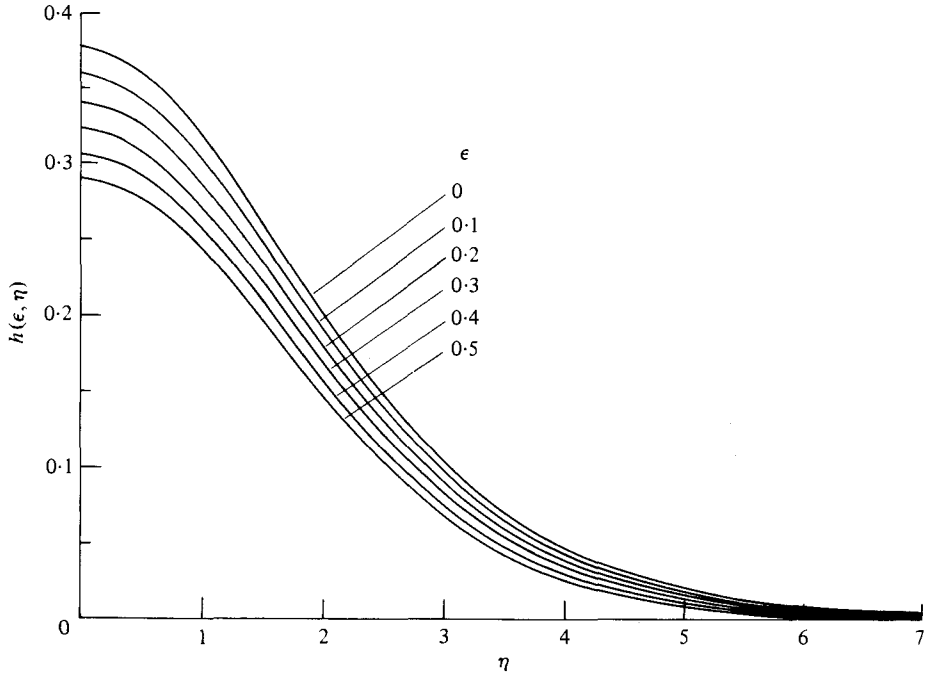

FIGURE 2. Favourable case: the temperature profiles from the first five terms of series (39) for a strongly buoyant plume.

For weakly buoyant two-dimensional plume the numerical results for first eleven terms in perturbation expansions for velocity $F'(\xi, 0)$ and temperature $H(\xi, 0)$ in the plane of symmetry and displacement thickness δ^* for $\sigma = 0{\cdot}72$ may be written as

$$F'(\xi, 0) = \sum_{n=0} a_n (\pm \xi)^n, \tag{55a}$$

$$H(\xi, 0) = \sum_{n=0} b_n (\pm \xi)^n, \tag{55b}$$

$$\delta^* = \sum_{n=0} d_n (\pm \xi)^{n+2}. \tag{55c}$$

The values of coefficients a_n, b_n and d_n are given in table 1. The results show that the convergences of these series are quite good for small values of ξ. The radius of convergence of the series ξ_0 defined by D'Alembert's ratio test is

$$\xi_0 = \lim_{n\to\infty} |a_{n-1}/a_n| \quad \text{or} \quad \xi_0 = \lim_{n\to\infty} |b_{n-1}/b_n|.$$

Domb & Sykes (1957) have observed that D'Alembert's limit can hopefully be estimated from a finite number of coefficients in series by plotting the inverse ratios a_n/a_{n-1} or b_n/b_{n-1} against $1/n$ (known as a Domb–Sykes plot) and extrapolating it to $1/n = 0$. The Domb–Sykes plots have the advantage that for certain common types of functions the extrapolation turns out to be linear. For example, for the following functions

$$F' = \text{const.} \times \begin{cases} (\xi_0 \pm \xi)^a, & a \neq 0, 1, \ldots, \\ (\xi_0 \pm \xi)^a \log (\xi_0 \pm \xi), & a = 0, 1, \ldots, \end{cases} \tag{56a, 56b}$$

	Coefficients of small-ξ series (55)			Coefficients of Eulerized series (60)		
n	a_n	b_n	d_n	A_n	B_n	D_n
0	1·0	0·239365	−0·5	0·828613	0·262957	−0·72822
1	0·258975	$-0{\cdot}125705\times10^{-1}$	0·14990	$0{\cdot}119047\times10^{-1}$	$0{\cdot}304963\times10^{-1}$	−0·23326
2	$-0{\cdot}51126\times10^{-1}$	$0{\cdot}301922\times10^{-2}$	$-0{\cdot}62529\times10^{-1}$	$-0{\cdot}187531\times10^{-2}$	$0{\cdot}135317\times10^{-1}$	−0·12870
3	$0{\cdot}174952\times10^{-1}$	$-0{\cdot}101311\times10^{-2}$	$0{\cdot}29566\times10^{-1}$	$-0{\cdot}236712\times10^{-2}$	$0{\cdot}809611\times10^{-2}$	$-0{\cdot}85516\times10^{-1}$
4	$-0{\cdot}722383\times10^{-2}$	$0{\cdot}397441\times10^{-3}$	$-0{\cdot}14940\times10^{-1}$	$-0{\cdot}205945\times10^{-2}$	$0{\cdot}556402\times10^{-2}$	$-0{\cdot}62568\times10^{-1}$
5	$0{\cdot}32893\times10^{-2}$	$-0{\cdot}170991\times10^{-3}$	$0{\cdot}78771\times10^{-2}$	$-0{\cdot}171255\times10^{-2}$	$0{\cdot}414197\times10^{-2}$	$-0{\cdot}48406\times10^{-1}$
6	$-0{\cdot}159151\times10^{-2}$	$0{\cdot}782146\times10^{-4}$	$-0{\cdot}42836\times10^{-2}$	$-0{\cdot}142580\times10^{-2}$	$0{\cdot}324713\times10^{-2}$	$-0{\cdot}38880\times10^{-1}$
7	$0{\cdot}802681\times10^{-3}$	$-0{\cdot}373848\times10^{-4}$	$0{\cdot}23639\times10^{-2}$	$-0{\cdot}120084\times10^{-2}$	$0{\cdot}263890\times10^{-2}$	$-0{\cdot}33000\times10^{-1}$
8	$-0{\cdot}417275\times10^{-3}$	$0{\cdot}184713\times10^{-4}$	$-0{\cdot}13252\times10^{-2}$	$-0{\cdot}102538\times10^{-2}$	$0{\cdot}220150\times10^{-2}$	$-0{\cdot}32088\times10^{-1}$
9	$0{\cdot}221987\times10^{-3}$	$-0{\cdot}936619\times10^{-5}$	$0{\cdot}75745\times10^{-3}$	$-0{\cdot}887858\times10^{-3}$	$0{\cdot}187289\times10^{-2}$	$-0{\cdot}39242\times10^{-1}$
10	$-0{\cdot}120264\times10^{-3}$	$0{\cdot}484946\times10^{-5}$	—	$-0{\cdot}779411\times10^{-3}$	$0{\cdot}161700\times10^{-2}$	—

TABLE 1. Coefficients in the series for velocity and temperature in the plane of symmetry and displacement thickness for weakly buoyant two-dimension plume (55) and their Euler transform (60).

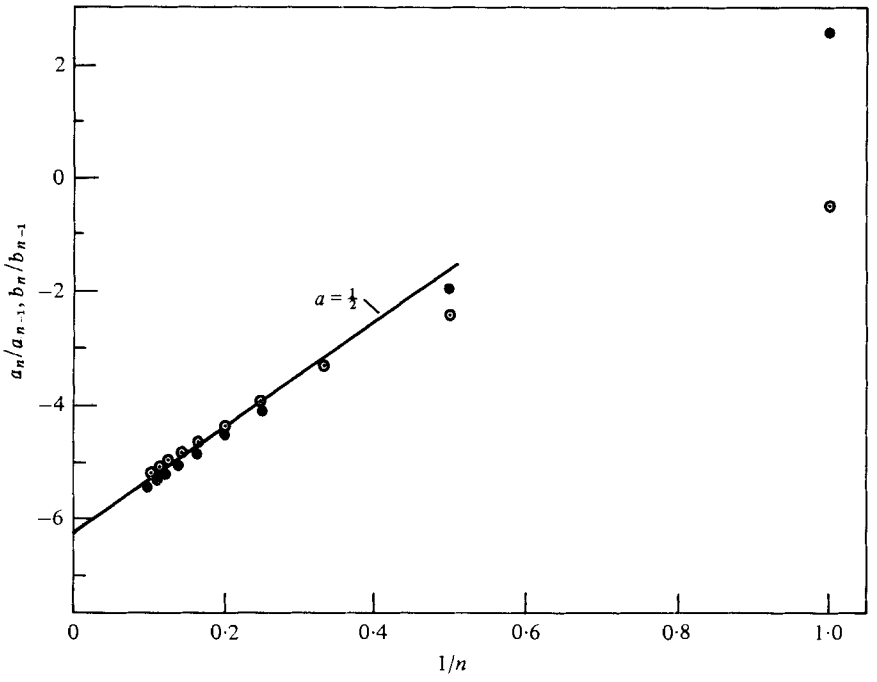

FIGURE 3. The Domb–Sykes plots for weakly buoyant plume series (55) for velocity and temperature in the plane of symmetry. ●, velocity; ○, temperature.

the inverse coefficient ratio in the expansion $F' = \Sigma a_n \xi^n$

$$\frac{a_n}{a_{n-1}} = \mp \frac{1}{\xi_0}\left(1 - \frac{1+a}{n}\right) \tag{57}$$

is exactly linear in $1/n$. For more complicated functions nearest singularity has a leading term like (56) and the ratio a_n/a_{n-1} will behave asymptotically linearly like (57) for large n. Thus for most of the functions generally encountered in practice the Domb–Sykes plots extrapolation to $1/n = 0$ is linear. The slope of the Domb–Sykes plot gives the nature of the singularity and the inverse of the intercept gives its location. Finally in making linear extrapolation for curved Domb–Sykes plots one naturally tends to favour slopes that correspond to simple values of exponents. The ratios of successive terms a_n/a_{n-1} and b_n/b_{n-1} for velocity and temperature in the plane of symmetry from expansions (55*a*) and (55*b*) are displayed against $1/n$ in figure 3. The Domb–Sykes plot for velocity is linear whereas for temperature it is curved. An extrapolation of the two Domb–Sykes plots to $1/n = 0$ yields slope a and intercept $1/\xi_0$ in expression (57) as

$$a = \tfrac{1}{2}, \quad \xi_0 = 1{\cdot}6. \tag{58}$$

These values are also consistent with the Domb–Sykes plot for displacement thickness series (55*c*). The series (55) possess the square-root singularity on the real axis in complex-ξ plane at $\xi = \pm \xi_0$. For the favourable case the square root singularity is on the negative real axis at $\xi = -\xi_0$, and for adverse case on the positive real axis at $\xi = \xi_0$. The use of various methods that accelerate the convergence often depend on the location of the nearest singularity and therefore the two cases demand separate treatment.

Let us first consider the favourable case, where the nearest singularity lies off the positive axis. As a singularity off the positive axis is of no physical interest, we can eliminate it by mapping it away to infinity by the Euler transformation

$$Z = \xi/(\xi+\xi_0). \tag{59}$$

In Eulerizing the series (55) we make use of the fact that for strongly buoyant plumes $\xi\to\infty$, $F'(\xi,0)\sim\xi^{\frac{2}{5}}$, $H(\xi,0)\sim\xi^{-\frac{1}{5}}$ and $\delta^*\sim\xi^{\frac{3}{5}}$. Now extracting the factors $\xi^{\frac{2}{5}}$, $\xi^{-\frac{1}{5}}$ and $\xi^{\frac{1}{5}}$ from the series (55) for velocity, temperature and displacement thickness respectively and recasting them in terms of variable Z, we get new series, which hopefully are also convergent for strongly buoyant plume,

$$F'(\xi,0)\,\xi^{-\frac{2}{5}} = \sum_{m=0} A_m Z^{m-\frac{2}{5}}, \tag{60a}$$

$$H(\xi,0)\,\xi^{\frac{1}{5}} = \sum_{m=0} B_m Z^{m+\frac{1}{5}}, \tag{60b}$$

$$\delta^*\xi^{-\frac{3}{5}} = \sum_{m=0}^{\infty} D_m Z^{m+\frac{4}{5}}. \tag{60c}$$

The coefficients A_m, B_m and D_m are also given in table 1. At $Z = 1$ the last partial sums of the series (60) for velocity, temperature and displacement thickness are 0·827, 0·336 and 1·43 whereas the corresponding exact results (54) for $\xi\to\infty$ are 0·80961, and 0·37728 and 2·0441. This shows that the last partial sum overestimates velocity at axis by 2 %, underestimates the temperature at the axis by 10% and displacement thickness by 32 %. The partial sums of the series can, hopefully, further be improved by the use of Shanks (1955) nonlinear transformation (which amounts to extrapolating on the assumption that the partial sums are a part of geometric sequence),

$$e_1(S_n) = \frac{S_{n+1}S_{n-1}-S_n^2}{S_{n+1}+S_{n-1}-2S_n}, \tag{61}$$

where S_n is the nth partial sum. The Shanks transformation to last three partial sums yields 0·823 for velocity and 0·350 for temperature. The corresponding percentage errors are 2 and 7 respectively.

A more systematic method of further improving the results is to explore the possibility of completing the series by finding the remainder. If the known coefficients of the series have settled down to display some sort of regular behaviour then the extrapolation to remainder terms can be carried out by assuming that the subsequent terms are proportional to those in the expansion of some known function whose coefficients have similar behaviour. Domb & Sykes (1957) have suggested that the completion of the series be made using simple functions of the form (56) indicated by their graphical ratio test. From the Eulerized series (60) the Domb–Sykes plots (i.e. A_n/A_{n-1} and B_n/B_{n-1} plotted against $1/n$) are displayed in figure 4. Because the signs of the coefficients are unchanged the nearest singularity in the Eulerized series now lies on the positive real axis in the complex-Z plane. The Domb–Sykes plot for temperature is curved, showing a regular behaviour, whereas for velocity there is a damped oscillation, which was invisible in figure 3, but has been enormously magnified in figure 4. Nevertheless, the intercept appears to be unity, showing that the radius of convergence of Eulerized series is unity for Z and hence infinite for ξ itself. The limiting slopes from the Domb–Sykes plot for temperature is $a = \frac{2}{5}$,

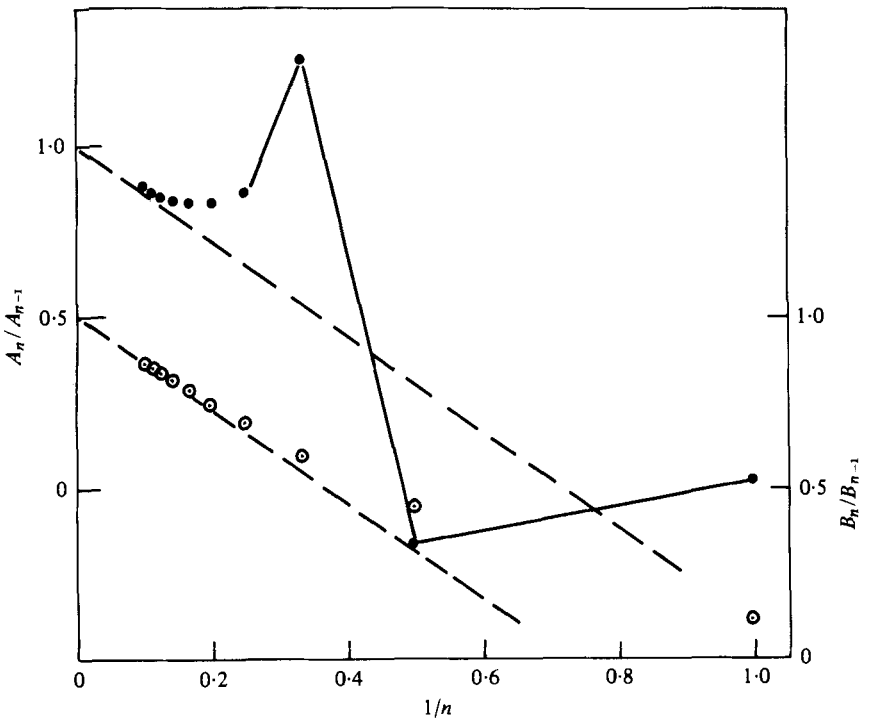

FIGURE 4. The Domb–Sykes plots for Eulerized series (60) for velocity and temperature in the plane of symmetry. ●, velocity; ○, temperature.

whereas for the velocity the oscillation complicates the problem. However, our study of the present problem for strongly buoyant plume ($\xi \to \infty$) carried out in § 4 shows

$$\xi^{-\frac{2}{5}} F'(\xi, 0) = 0{\cdot}8091 + 0{\cdot}06312\xi^{-\frac{2}{5}} + \ldots \quad \text{as} \quad \xi \to \infty,$$

implying that the next term has a slope of $\frac{2}{5}$ as $\xi \to \infty$. A straight line with slope $a = \frac{2}{5}$ and intercept of unity also displayed in figure 4 on the Domb–Sykes plot for the velocity shows that the curve for large n approaches the straight line. Thus in the Eulerized series (60) the remainder for the sum can be taken proportional to that in the expansion of $(1-z)^{\frac{2}{5}}$. The constants of proportionality are chosen so that the coefficients of the last term z^N are equal. Thus the completed series for velocity and temperature at the axis and displacement thickness are

$$F'(\xi, 0)\,\xi^{-\frac{2}{5}} = Z^{-\frac{2}{5}}\left[\sum_{n=0}^{9} A_n Z^n + A_{10} R_{10}\right],$$

$$H(\xi, 0)\,\xi^{\frac{1}{5}} = Z^{\frac{1}{5}}\left[\sum_{n=0}^{9} B_n Z^n + B_{10} R_{10}\right],$$

$$\delta^* \xi^{-\frac{6}{5}} = Z^{\frac{4}{5}}\left[\sum_{n=0}^{7} D_n Z^n + D_8 R_8\right],$$

where the R_m is the remainder given by

$$R_m = \left[(1-Z)^{\frac{2}{5}} - \sum_{n=0}^{m} \binom{\frac{2}{5}}{n} (-Z)^n\right] \Big/ \binom{\frac{2}{5}}{m}.$$

	Coefficients of completed Eulerized series (62)			Coefficients of low ξ completed series (6 4)		
n	$\mathscr{A}_n$	$\mathscr{B}_n$	$\mathscr{D}_n$	a_n	b_n	d_n
-1	0·070814	$-0·146915$	2·11723	1·424909	$-0·574973\times10^{-1}$	$-4·771005$
0	0·757799	0·409872	$-2·84546$	$-0·425909$	0·296863	5·271005
1	$0·402304\times10^{-1}$	$-0·282694\times10^{-1}$	0·61363	$-0·186617$	$0·539741\times10^{-2}$	1·341039
2	$0·662239\times10^{-2}$	$-0·409804\times10^{-2}$	0·12537	$0·184981\times10^{-1}$	$0·211732\times10^{-3}$	$-0·170430$
3	$0·216499\times10^{-2}$	$-0·130641\times10^{-2}$	$0·49986\times10^{-1}$	$-0·426239\times10^{-2}$	$-0·135775\times10^{-3}$	$0·432341\times10^{-1}$
4	$0·886424\times10^{-3}$	$-0·547620\times10^{-3}$	$0·25508\times10^{-1}$	$0·127525\times10^{-2}$	$0·547305\times10^{-4}$	$-0·134978\times10^{-1}$
5	$0·408477\times10^{-3}$	$-0·258411\times10^{-3}$	$0·15020\times10^{-1}$	$-0·429007\times10^{-3}$	$-0·210550\times10^{-4}$	$0·456423\times10^{-2}$
6	$0·200318\times10^{-3}$	$-0·126495\times10^{-3}$	$0·97379\times10^{-2}$	$0·151462\times10^{-3}$	$0·793210\times10^{-5}$	$-0·154824\times10^{-2}$
7	$0·100058\times10^{-3}$	$-0·600005\times10^{-4}$	$0·58939\times10^{-2}$	$-0·532445\times10^{-4}$	$-0·287108\times10^{-5}$	$0·499966\times10^{-3}$
8	$0·478534\times10^{-4}$	$-0·250894\times10^{-4}$	—	$0·173742\times10^{-4}$	$0·944801\times10^{-6}$	$-0·129161\times10^{-3}$
9	$0·184331\times10^{-4}$	$-0·734482\times10^{-5}$	—	$-0·439290\times10^{-5}$	$-0·237803\times10^{-6}$	—

TABLE 2. Coefficients in the series for velocity and temperature in the plane of symmetry and displacement thickness for two-dimensional buoyant plume of completed Eulerized series (62) and completed low ξ series (64).

The coefficients of the remainder terms can be chosen such that the last (eleventh) term in the Eulerized and completed series are equal. However, for the displacement thickness δ^* the Eulerized series (60*c*) along with table 1 show that the magnitude of the last term D_9 is greater than the preceding terms. Therefore, following Van Dyke (1964, p. 31), we have stopped the series (60*c*) at D_8 and completed it at this stage itself. The results for the completed series are

$$F'(\xi,0)\,\xi^{-\frac{2}{5}} = Z^{-\frac{2}{5}}\left[\mathscr{A}_{-1}(1-Z)^{\frac{2}{5}} + \sum_{m=0}^{9}\mathscr{A}_m Z^m\right], \tag{62a}$$

$$H(\xi,0)\,\xi^{\frac{1}{5}} = Z^{\frac{1}{5}}\left[\mathscr{B}_{-1}(1-Z)^{\frac{2}{5}} + \sum_{m=0}^{9}\mathscr{B}_m Z^m\right], \tag{62b}$$

$$\delta^*\xi^{-\frac{6}{5}} = Z^{\frac{4}{5}}\left[\mathscr{D}_{-1}(1-Z)^{\frac{2}{5}} + \sum_{m=0}^{7}\mathscr{D}_m Z^m\right], \tag{62c}$$

where coefficients $\mathscr{A}_m$, $\mathscr{B}_m$ and $\mathscr{D}_m$ are also given in table 2. As $Z\to 1$ ($\xi\to\infty$) the completed Eulerized series (62) yield

$$F'(\xi,0)\,\xi^{-\frac{2}{5}} = 0{\cdot}8085, \tag{63a}$$

$$H(\xi,0)\,\xi^{\frac{1}{5}} = 0{\cdot}3752, \tag{63b}$$

$$\delta^*\xi^{-\frac{6}{5}} = -2{\cdot}0003, \tag{63c}$$

whereas the corresponding exact results given by (64) are 0·8096, 0·3773 and −2·0441. Thus when $\xi\to\infty$ the results (63) underestimate velocity by 0·2 %, temperature by 0·8 % and displacement thickness by 2·2 %.

Finally, the series (55) for weakly buoyant plume can also be completed with the help of Domb–Sykes plot given in figure 3. The slope of the plots correspond to $a = \frac{1}{2}$ and the intercept to $\xi_0 = 1{\cdot}6$. The remainder in these series can be taken proportional to $(\xi_0+\xi)^{\frac{1}{2}}$ and the series completed are

$$F'(\xi,0) = a_{-1}(1+\xi/\xi_0)^{\frac{1}{2}} + \sum_{m=0}^{9} a_m\,\xi^m, \tag{64a}$$

$$H(\xi,0) = \ell_{-1}(1+\xi/\xi_0)^{\frac{1}{2}} + \sum_{m=0}^{9} \ell_m\,\xi^m, \tag{64b}$$

$$\delta^* = \xi^2\left[d_{-1}(1+\xi/\xi_0)^{\frac{1}{2}} + \sum_{m=0}^{8} d_m\,\xi^m\right], \tag{64c}$$

with the coefficients a_m, ℓ_m and d_m given in table 2. It may be noted that coefficients of series (64) are greatly reduced and converge much faster with greater radius of convergence when compared with the original series (55).

The results for velocity and temperature in the plane of symmetry and displacement thickness obtained from completed Eulerized series 62(*a–c*) are displayed against ξ, in figures 5(*a–c*) respectively. On the respective figures, the results of completed series (64), asymptotes for small and large ξ and sum of first five terms in large ξ series (54) are also displayed. Figure 4 shows that the reliance on the asymptote for large ξ is good when $\xi > 50$ for velocity, $\xi > 500$ for temperature and $\xi > 1000$ for displacement thickness. The first five terms of large ξ series (54) are very good for $\xi \gtrsim 10$. The completed low ξ series (64) are good for $\xi \lesssim 3$. It is interesting

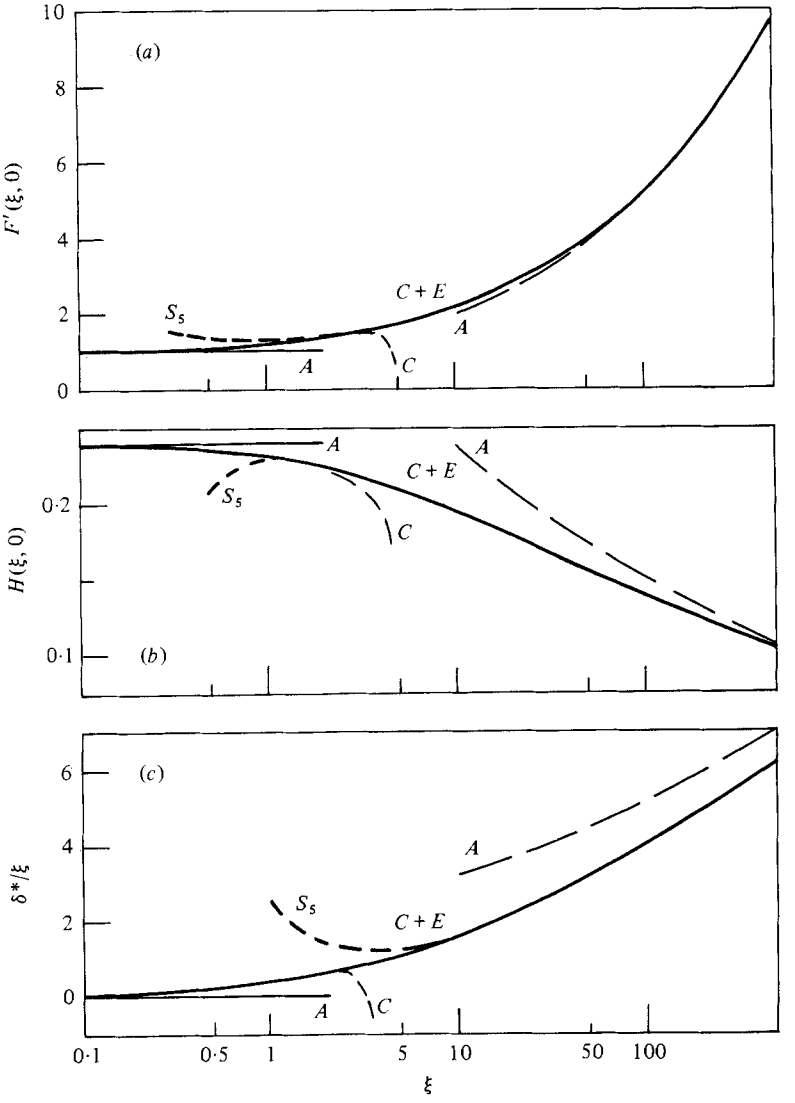

FIGURE 5. Favourable case: the comparison of various characteristics for mixed convection buoyant plume. (*a*) Velocity $F'(\xi, 0)$ in the plane of symmetry. (*b*) Temperature $H(\xi, 0)$ in the plane of symmetry. (*c*) Displacement thickness δ^*. $C+E$: the completed Eulerized series (62), C: the completed series (64), A: the asymptotes for small and large values of ξ. S_5: the sum of first five terms in large ξ series (54).

to note that predictions based on completed Eulerized series (62) are extremely good throughout the domain shown in figure 5. When $\xi \to \infty$ the completed Eulerized series underestimates velocity by 0·2%, temperature by 0·8% and displacement thickness by 2·2%.

The numerical results of velocity and temperature profiles given by expressions (15) can be estimated for various values of ξ as well, but their utility will be limited for $\xi < 1$, due to their limited radius of convergence. Therefore, using the Domb–Sykes plot of figure 3, the series (15) for velocity and temperature profiles are Eulerized for

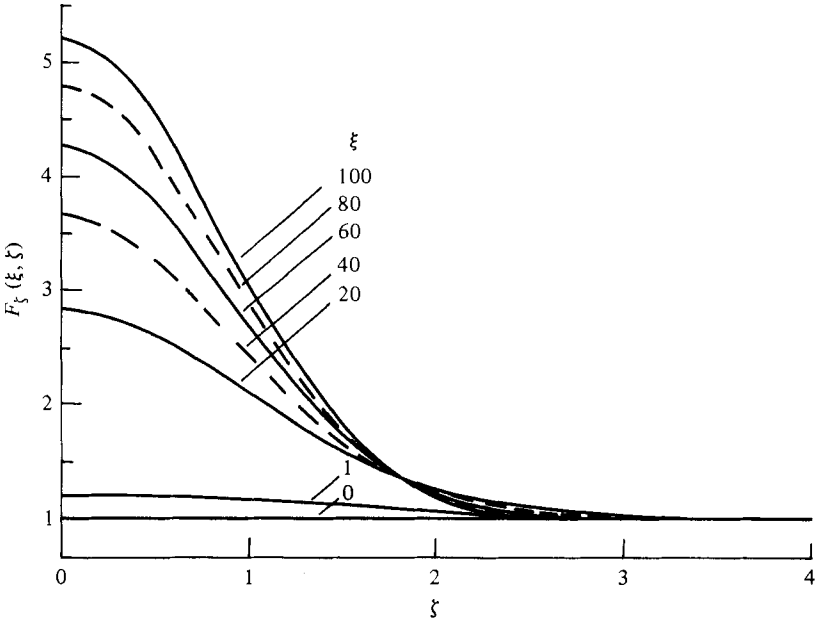

FIGURE 6. Favourable case: the velocity profiles from completed Eulerized series (65) with streamwise distance ξ as a parameter.

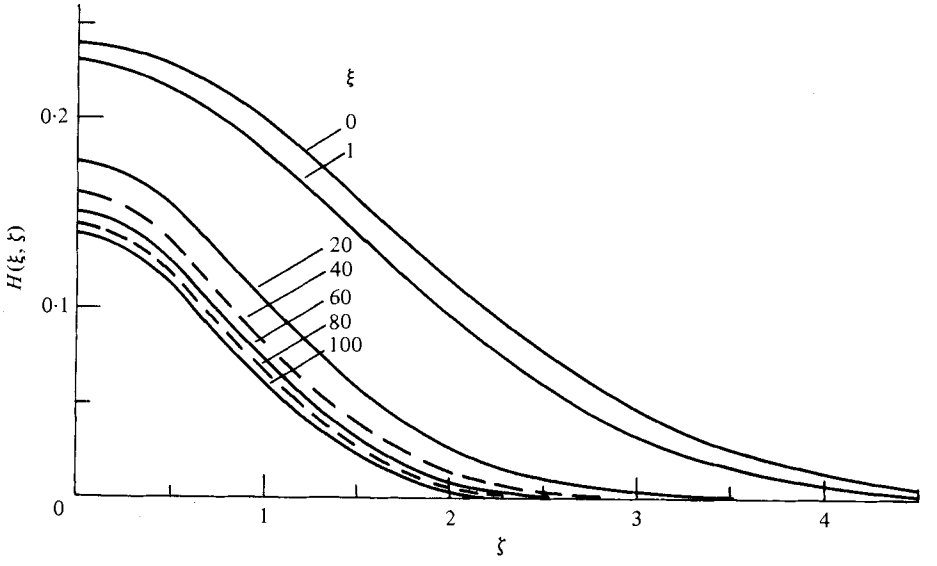

FIGURE 7. Favourable case: the temperature profiles from completed Eulerized series (66) with streamwise distance ξ as a parameter.

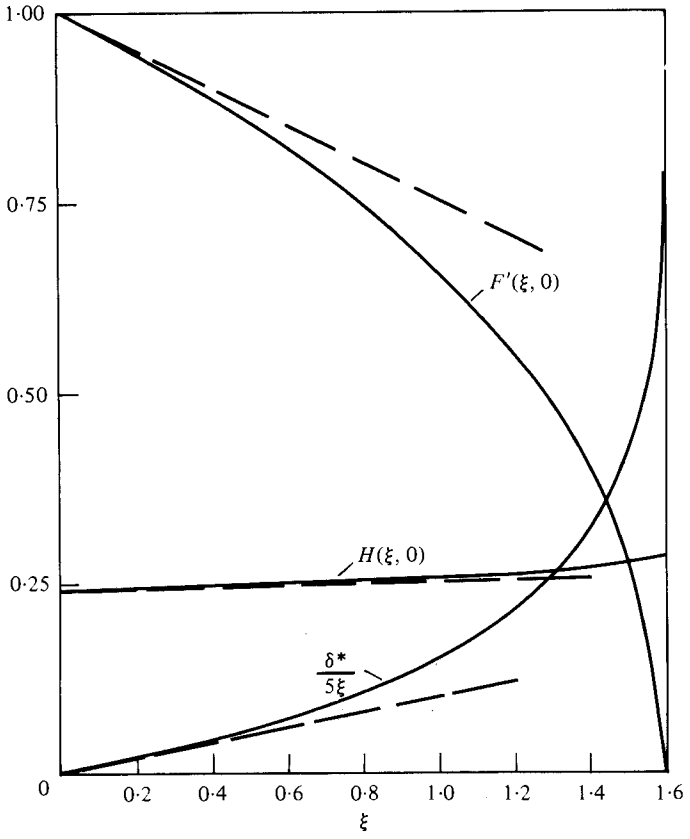

FIGURE 8. Adverse case: the characteristics of mixed convection plume when forced convection and buoyancy effects oppose each other. $F'(\xi, 0)$, velocity at axis. $H(\xi, 0)$, temperature at axis, δ^*, the displacement thickness. —— completed series. – – – Oseen approximation.

every value of ζ and these Eulerized series are subsequently completed by using the Domb–Sykes plot of figure 4 to yield

$$F_\zeta(\xi, \zeta) = (\xi/Z)^{\frac{2}{5}}\left[\mathscr{F}'_{-1}(\zeta)(1-Z)^{\frac{2}{5}} + \sum_{m=0}^{9} \mathscr{F}'_m(\zeta) Z^m\right], \tag{65}$$

$$H(\xi, \zeta) = (\xi/Z)^{-\frac{1}{5}}\left[\mathscr{H}_{-1}(\zeta)(1-Z)^{\frac{2}{5}} + \sum_{m=0}^{9} \mathscr{H}_m(\zeta) Z^m\right]. \tag{66}$$

Here $\mathscr{F}'$ and $\mathscr{H}$ obtained from completion of the series at the eleventh term are

$$\mathscr{F}'_{-1}(\zeta) = -\hat{F}'_{10}(\zeta) \Big/ \binom{\frac{2}{5}}{10}, \tag{67a}$$

$$\mathscr{F}'_m(\zeta) = \hat{F}'_m(\zeta) + \mathscr{F}'_{-1}(\zeta)\binom{\frac{2}{5}}{m}(-1)^m, \tag{67b}$$

$$\mathscr{H}_{-1}(\zeta) = -\hat{H}_{10}(\zeta) \Big/ \binom{\frac{2}{5}}{10}, \tag{68a}$$

$$\mathscr{H}_m(\zeta) = \hat{H}_m(\zeta) + \mathscr{H}_{-1}(\zeta)\binom{\frac{2}{5}}{m}(-1)^m. \tag{68b}$$

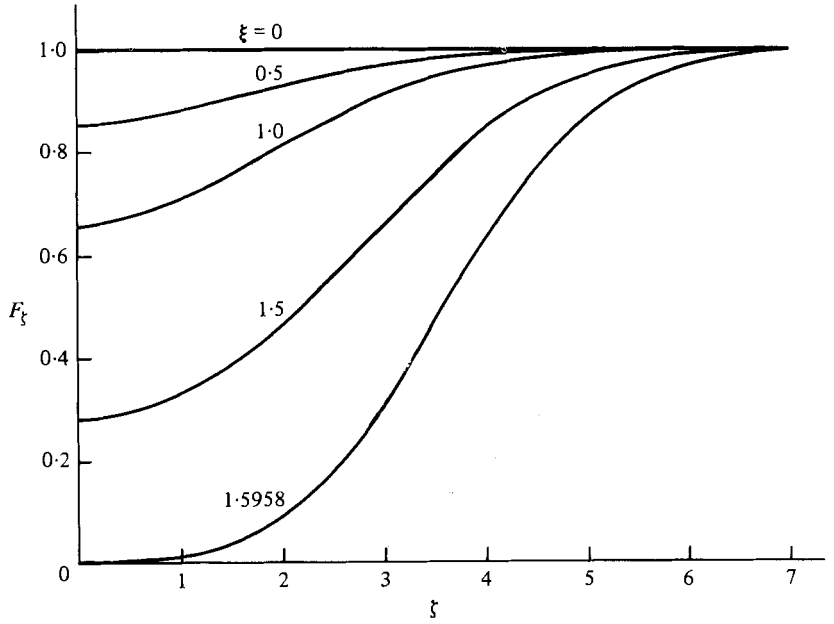

FIGURE 9. Adverse case: the profiles of velocity from completed series with ξ as a parameter.

The coefficients $\hat{F}'_m$ and $\hat{H}_m$ are connected to the coefficients of the series (15) by the relations

$$\hat{F}'_m(\zeta) = \sum_{n=0}^{m} \binom{m-\frac{3}{5}}{m-n} F'_n(\zeta)\, \xi_0^{n+\frac{2}{5}}, \tag{69a}$$

$$\hat{H}_m(\zeta) = \sum_{n=0}^{m} \binom{m-\frac{6}{5}}{m-n} H_n(\zeta)\, \xi_0^{n-\frac{1}{5}}, \tag{69b}$$

and

$$\binom{a}{b} = \frac{\Gamma(a+1)}{\Gamma(b+1)\,\Gamma(a-b+1)}. \tag{70}$$

The coefficients $\mathscr{F}'_m$ and $\mathscr{H}_m$ of completed Eulerized series (65) and (66) for velocity and temperature profiles estimated from solutions for expansions (15) are given in tables 3 and 4.† The velocity and temperature profiles calculated from the coefficients of completed Eulerized series (65) and (66) are displayed against normal co-ordinate ζ in figures 6 and 7 for typical values of $\xi = 0$, 1, 20, 40, 60, 80 and 100. These profiles show that as ξ becomes large the thickness of the buoyancy layer becomes very small and the appropriate normal co-ordinate is η given by (36a) rather than ζ. For further higher values of ξ the profiles for velocity and temperature for various values of $\zeta(=\eta\xi^{\frac{1}{5}})$ may be estimated from tables 3 and 4 or also may be directly obtained from figures 1 and 2.

We now present our results for the adverse case. The nearest singularity in the complex-ξ plane lies on the positive axis at $\xi = \xi_0$, in the domain of interest. In general, there is no question of eliminating it, short of refining the whole theory. However, in the present case the square root on the positive axis is not a real

† These tables are available upon request from the Editorial Office.

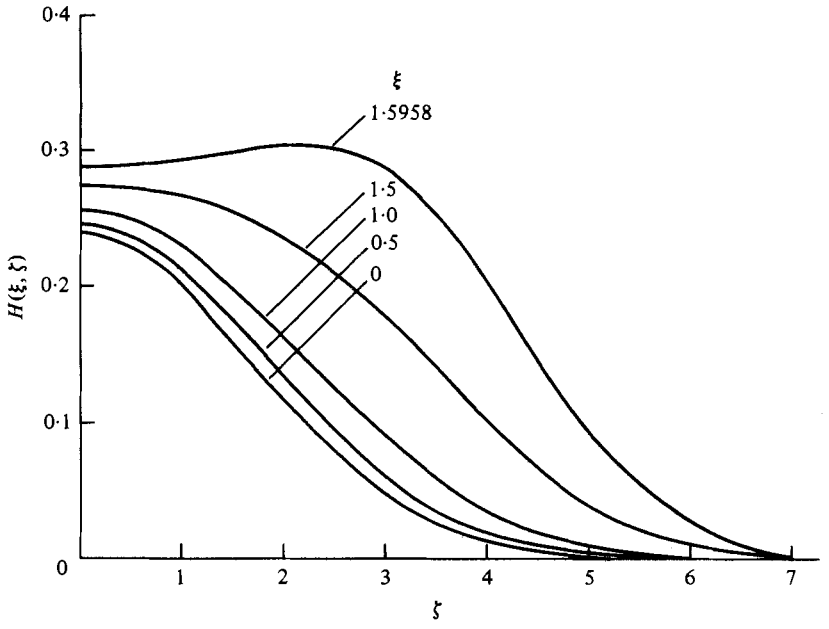

FIGURE 10. Adverse case: The profiles of temperature from completed series with ξ as a parameter.

singularity, but an indication that the function is double-valued (Van Dyke 1974). The dual solutions correspond to the forward and reverse flows in the plume. For the forward flow the extraction of the nearest singularity by subtraction from series (55), yields the series that are identical with (64) except that ξ is replaced by $-\xi$. The results so obtained from the completed series for velocity and temperature in the plane of symmetry and displacement thickness are displayed in figure 8 against the mixed convection parameter ξ. Figure 8 shows that as ξ increases the velocity at the axis decreases. As ξ approaches ξ_0 the buoyant force opposes the forced convection flow so much that the axial velocity approaches zero (at $\xi = 0{\cdot}1598 \simeq \xi_0$, $F'(\xi_0, 0) = 0$). The figure also shows that the thickness of the plume increases with ξ. The velocity and temperature profiles (15) can also be obtained by subtraction of singularity by a method similar to that employed in (65)–(70). The profiles of velocity and temperature so obtained are displayed in figures 9 and 10 with ξ as a parameter, which clearly show the nature of the solutions discussed above.

From the above it is clear how the analysis of weakly buoyant plumes can yield almost complete characterization of the solutions in the entire complex plane of the parameter ξ (or ϵ) representing the mixed convection effects. The nature and location of the singularities have been found and by judicious recasting the series we have been able to get two-figure accuracy even for strongly buoyant plumes. Thus the completed Eulerized series for weakly buoyant plumes predicts extremely accurate results even for strongly buoyant plumes.

Appendix

We here describe a method for determining the constant c_1. The solutions f_5 and h_5 of equations (50) and (51) are of the form

$$f_5 = x_a + c_1 x_b + A x_c + B x_d + \lambda f_{5c}, \tag{A 1}$$

$$h_5 = \phi_a + c_1 \phi_b + A \phi_c + B \phi_d + \lambda h_{5c}. \tag{A 2}$$

The (x_a, ϕ_a) and (x_b, ϕ_b) are the particular integrals satisfying the following equations

$$L(x_a, \phi_a) = R_5, \quad \mathscr{L}(x_a, \phi_a) = \mathscr{R}_5, \tag{A 3}$$

$$L(x_b, \phi_b) = (3 f_0 f_0'' - f_0'^2)/10, \quad \mathscr{L}(x_b, \phi_b) = 3(f_0' h_0 - f_0 h_0')/10, \tag{A 4}$$

with the following boundary conditions

$$x_a'(0) = \phi_a(0) = x_b'(0) = \phi_b = 0. \tag{A 5}$$

The complementary functions (x_c, ϕ_c) and (x_d, ϕ_d) satisfy the following equations

$$L(x_c, \phi_c) = \mathscr{L}(x_c, \phi_c) = 0; \quad L(x_d, \phi_d) = \mathscr{L}(x_d, \phi_d) = 0, \tag{A 6}$$

together with the boundary conditions

$$x_c'(0) = 1, \quad \phi_c(0) = 0; \quad x_d'(0) = 0, \quad \phi_d(0) = 1. \tag{A 7}$$

In the above solution λ is an unspecified constant and (f_{5c}, h_{5c}) is the complementary function which arises owing to the eigenvalue of the operators. The addition of this solution does not affect the boundary conditions or equations. A solution may be chosen which satisfies the following condition

$$f_{5c}'(0) = f_0'(0), \quad h_{5c}(0) = -h_0(0),$$

and may be written as

$$f_{5c} = 3 f_0 - 2\eta f_0', \quad h_{5c} = -(h_0 + \tfrac{2}{3}\eta h_0'). \tag{A 8}$$

The solution (f_{5c}, h_{5c}) can also be written in terms of x_c and x_d as

$$f_{5c} = f_0'(0)\, x_c - h_0(0)\, x_d, \quad h_{5c} = f_0'(0)\, \phi_c - h_0(0)\, \phi_d.$$

As f_{5c}' and h_{5c} go to zero as $\eta \to \infty$ we get

$$\frac{\phi_d(0)}{\phi_c(0)} = \frac{x_d'(0)}{x_c'(0)} = \frac{f_0'(0)}{h_0(0)}. \tag{A 9}$$

An analysis of the equations governing complementary functions and particular integrals for large values of η leads to

$$\phi_i \sim Q_i, \quad X_i \sim -\frac{3 Q_i \eta^2}{10 f_0(\infty)} + P_i \eta + M_i, \tag{A 10}$$

where $i = a, b, c, d$ and Q_i, P_i and M_i are constants. The temperature and velocity at infinity are given by

$$\left.\begin{aligned} h_5(\infty) &= Q_a + c_1 Q_b + A Q_c + B Q_d, \\ f_5'(\infty) &= P_a + c_1 P_b + A P_c + B P_d - 0{\cdot}6 h_5(\infty)/f_0(\infty), \end{aligned}\right\} \tag{A 11}$$

and the condition (A 10) yields

$$\frac{Q_d}{Q_c} = \frac{P_d}{P_c} = \frac{f_0'(0)}{h_0(0)}. \tag{A 12}$$

Now, satisfying the boundary conditions $h_5(\infty) = f_5'(\infty) = 0$, we get

$$\left.\begin{aligned} A + Bf_0'(0)/h_0(0) &= -(P_a + c_1 P_b)/P_c, \\ A + Bf_0'(0)/h_0(0) &= -(Q_a + c_1 Q_b)/Q_c, \end{aligned}\right\} \tag{A 13}$$

which are consistent provided

$$c_1 = \frac{P_c Q_a - F_a Q_c}{P_b Q_c - Q_b P_c}. \tag{A 14}$$

The equations (A 13) yield an equation

$$A + Bf_0'(0)/h_0(0) = -(P_a + c_1 P_b)/P_c = -(Q_a + c_1 Q_b)/Q_c$$

in terms of two constants A and B. In view of the fact that an unspecified constant λ is included in the solutions one of the constants can be taken as zero, say $B = 0$. The expression for displacement thickness is

$$f_5(\infty) = M_a + c_1 M_b + A M_c + \lambda f_{5c}(\infty). \tag{A 15}$$

A numerical integration for the equations for $\sigma = 0{\cdot}72$ leads to

$$\left.\begin{aligned} c_1 &= -1{\cdot}0728, \quad A = -1{\cdot}03385, \\ f_5'(0) &= -1{\cdot}03385 + 0{\cdot}80961\lambda, \\ h_5(0) &= -0{\cdot}37728\lambda, \\ f_5(\infty) &= -11{\cdot}8579 + 6{\cdot}13221\lambda. \end{aligned}\right\} \tag{A 16}$$

REFERENCES

Domb, C. & Sykes, M. F. 1957 On the susceptibility of a ferromagnetic above the Curie point. *Proc. Roy. Soc.* A **240**, 214–228.

Erdélyi, A. 1953 *Higher Transcendental Functions*, vols. 1 and 2. McGraw-Hill.

Fuji, T. 1963 The theory of the steady laminar natural convection above a horizontal line heat source and a point heat source. *Int. J. Heat Mass Transfer* **6**, 597–606.

Shanks, D. 1955 Nonlinear transformations of divergent and slowly convergent sequences. *J. Math. Phys.* **34**, 1–42.

Van Dyke, M. 1964 *Perturbation Methods in Fluid Mechanics*. Academic.

Van Dyke, M. 1974 Analysis and improvement of perturbation series. *Quart. J. Mech. Appl. Math.* **27**, 423–450.

Wesseling, P. 1974 An asymptotic solution for slightly buoyant plume. *J. Fluid Mech.* **70**, 81–87.

Wood, W. W. 1972 Free and forced convections from fine hot wires. *J. Fluid Mech.* **55**, 419–438.